Supporting Information for "Direct observation of the potential distribution organic light emitting diodes under operation"

Christian S. Weigel, Wolfgang Kowalsky and Rebecca Saive

Kelvin probe measurements and orientation polarization Previous Kelvin probe investigations of Alq_3 films have shown a constant surface potential increase with film thickness (up to 5 V per 100 nm) that is linked to spontaneous orientation polarization of the polar Alq_3 molecules but vanishes for various external stresses such as visible light or elevated temperature.[1,2] This permanent polarization density is around -1 mC/m^2.[3–6] SKPM measurements reproduced the surface potential shift on bare Alq_3 films as well as in the areas that had been behind a shadow mask during metal evaporation. It corresponds to the potential of the film surface against the substrate in the case of depletion at the transition voltage. After deposition of a metal contact onto the Alq_3 layer no such shift was found neither on the metal surface (before FIB cutting) nor in the Alq_3 beneath (after FIB cutting with floating top contact). This means that deposition of a metal layer on top of the Alq_3 film triggers compensation of the orientation polarization by charge accumulation.

SKPM raw data

The SEM image of the cross section of an OLED was captured by a high resolution and therefore high dose electron beam after exposure of the cross section but before the polishing to avoid electron beam damage to the final, polished cross section. After a final polishing step the probe tip was positioned at the edge of the milled hole using the SEM with high scan rate to avoid carbon deposition. Subsequently, topography and SKPM images were taken. The SEM allowed for accurate identification of the different layers and alignment and calibration of the SPM. The electron beam was blanked for further data acquisition.

Figure S1 shows the CPD profiles across the cross section of an OLED with an active layer of 224 nm Alq_3 and a) 224 nm NPB and b) 112 nm NPB at external bias voltage between a) -10 V and 5 V and b) -10 V and +10 V. The Al contact was kept on ground potential and the bias voltage was applied to the ITO contact. The 0 V profiles correspond to the work function difference between the cantilever tip and the sample. As electrostatic force is long-range, not only the very end of the probe tip interacts with the sample. The measured signal is also influenced by the sample interaction with the whole cantilever.[7–9] Although contacted to ground potential the measured CPD at the Al contact slightly changes its value upon different biases on the ITO. The corresponding measurement artifact on the ITO contact is even more pronounced because the FIB milled hole is significantly smaller than the cantilever so that most of the cantilever is positioned above and interacting with the Al contact. Therefore, the measured potential at the ITO contact is skewed towards the potential of the Al contact and smaller than the applied bias voltage. To facilitate the comparison of predicted and measured values shown in Fig. 2, we accounted for this measurement artifact by setting the ITO and Al on the nominal applied potential and extending the data in between.

The potential is constant along the anode and the top of the cathode and drops mainly across the organic layers. From this raw data it can already be seen that for small applied voltages the potential drops exclusively along the Alq_3 layer and only for bias voltages higher than the U_{trans}, there is also potential drop within the NPB layer. This behavior was discussed extensively in the results section.

Theory details Calculations of the potential distribution were conducted under the following assumptions: (1) With no free charge carriers in the device, any backwards bias in excess of the transition voltage is split among the two organic layers as in a plate capacitor with two stacked dielectrics. (2) Between the transition voltage and the onset voltage the voltage drop occurs only over the Alq_3 layer as localized hole accumulation overcomes negative polarization charge.[3,6] (3) Exceeding the onset voltage, electron injection and recombination occur. Further charge accumulation superimposes the existing accumulated charge. Two limiting cases are considered: (a) Current density is limited by injection through Schottky junctions at the electrodes.[10] In this case constant electric field is considered throughout each film and the respective potential drops across the layers are calculated from fits to I-V curves. (b) Only the difference in mobility values between electrons in Alq_3 and holes in NPB lead to additional charge accumulation at the interface.[3] The potential profiles in this case are described by space charge limited current theory. The dashed lines in Fig. 1 are calculated according to model (3a).

The following details the approach to analytically calculate the partial voltage drop across each layer n in the device. In the estimate that both contacts are considered ohmic[11] and traps are neglected, space charge limited current density ($j_{SCLC,n}$) across both layers can be assumed to match. Neglecting field dependence of the mobility, traps and electrical doping this can be described by the law of Mott and Gurney[12]:

$$j_{\mathrm{SCLC,n}} = \frac{9}{8}\varepsilon_{\mathrm{r,n}}\varepsilon_0\mu_{\mathrm{x}}\frac{{U_n}^2}{{d_n}^3}$$

$$\frac{U_{\mathrm{Alq3}}}{U_{\mathrm{NPB}}} = \left(\frac{d_{\mathrm{Alq3}}^3}{d_{\mathrm{NPB}}^3}\frac{\mu_{\mathrm{NPB}}\ \varepsilon_{\mathrm{r,NPB}}}{\mu_{\mathrm{Alq3}}\ \varepsilon_{\mathrm{r,Alq3}}}\right)^{\frac{1}{2}}$$

where U_n, d_n, μ_n, and $\varepsilon_{r,n}$ represent partial voltage drop, thickness, majority carrier mobility and relative permittivity across each layer ($n \in$ [Alq, NPB]). The relative permittivity was

considered equal for both materials $\varepsilon_{r,Alq3} = \varepsilon_{r,NPB}$. ε_0 is the vacuum permittivity. The hole mobility of NPB is approximately two orders of magnitude higher than the electron mobility of Alq_3.[13,14] Thus beyond the onset voltage, the partial potential drop across the Alq_3 layer is expected to be approximately 10 (30) times that across an equally thick (half as thick) NPB layer. In the SCLC approximation, the charge distribution follows an inverse square root behavior with the distance from the injecting electrode and the potential accordingly changes with a 3/2 exponential.

For Matsumura's model, the parameter for electron injection from LiF/Al into Alq_3 (zero-field injection current $J_{0,1}$) was taken from their study.[10] The equivalent parameter for hole injection $J_{0,2}$ and the built-in voltage U_{bi} were derived from fitting the I-V curves of the LiF devices to the model of current density J at room temperature T with elementary charge e and Boltzmann's constant k:

$$\ln J = \left(\frac{e^3 (U - U_{bi})}{(4\pi\varepsilon_r\varepsilon_0(d_1 + d_2)k^2T^2)} - \frac{d_1 d_2}{d_1 + d_2} \left(\ln \frac{J_{0,1}}{J_{0,2}} \right)^2 \right)^{\frac{1}{2}} + \frac{d_1}{d_1 + d_2} \ln J_{0,1} + \frac{d_2}{d_1 + d_2} \ln J_{0,2}$$

where d_1 and d_2 are the thickness of Alq_3 and NPB layer respectively and U is the applied bias across the device. The curves are presented in Fig. S2 and the obtained parameters are given in Table S1. The value obtained for the zero volt injection current $J_{0,2}$ of NPB on ITO/MoO_3 (0.053 A) corresponds well to Matsumura's value for TPD on ITO (0.017 A). The built-in voltage U_{bi} of approximately 1.20 V obtained from the fit (ITO/MoO_3 vs. LiF/Al) also agrees well with 1.15 V published (ITO vs. LiF/Al). Partial potential drops U_n were calculated by equating the currents through the single layers according to the fit parameters.

$$\ln J = \left(\frac{e^3 (U_n)}{(4\pi\varepsilon_{r,n}\varepsilon_0 d_n k^2 T^2)} \right)^{\frac{1}{2}} + \ln J_{0,n}$$

Table S1 Parameters for Schottky model.

parameter	value
$\varepsilon_{r,Alq3} = \varepsilon_{r,NPB}$	1 [15]
$J_{0,e}$	0.0032 A [16]
$J_{0.h}$	0.053 A (fit)
U_{bi}	1.198 V (fit)

References

[1] E. Ito, Y. Washizu, N. Hayashi, H. Ishii, N. Matsuie, K. Tsuboi, Y. Ouchi, Y. Harima, K. Yamashita, K. Seki, *J. Appl. Phys.* **2002**, *92*, 7306.

[2] N. Kajimoto, T. Manaka, M. Iwamoto, *J. App. Phys.* **2006**, *100*, 053707.

[3] S. Berleb, W. Brütting, G. Paasch, *Org. Electron* **2000**, *1*, 41.

[4] D. Y. Kondakov, J. R. Sandifer, C. W. Tang, R. H. Young, *J. App. Phys.* **2002**, *93*, 1108.

[5] Y. Noguchi, N. Sato, Y. Tanaka, Y. Nakayama, H. Ishii, *Appl.Phys. Lett.* **2008**, *92*, 203306.

[6] Y. Noguchi, Y. Miyazaki, Y. Tanaka, N. Sato, Y. Nakayama, T. D. Schmidt, W. Brütting, H. Ishii, *J. App. Phys.* **2012**, *111*, 114508.

[7] D. S. H. Charrier, M. Kemerink, B. E. Smalbrugge, T. de Vries, R. A. J. Janssen, *ACS Nano* **2008**, *2*, 622.

[8] E. Strassburg, A. Boag, Y. Rosenwaks, *Rev. Sci. Instrum.* **2005**, *76*, 083705.

[9] G. Elias, T. Glatzel, E. Meyer, A. Schwarzman, A. Boag, Y. Rosenwaks, *Beilstein J. Nanotechnology* **2011**, *2*, 252.

[10] M. Matsumura, A. Ito, Y. Miyamae, *Appl. Phys. Lett.* **1999**, *75*, 1042.

[11] M. Stößel, J. Staudigel, F. Steuber, J. Blässing, J. Simmerer, A. Winnacker, *Appl. Phys. Lett.* **2000**, *76*, 115.

[12] N. F. Mott, R. W. Gurney, *Electronic Processes in Ionic Crystals*, Clarendon Press, **1948**.

[13] T.-Y. Chu, O.-K. Song, *App. Phys. Lett.* **2007**, *90*, 203512.

[14] J. J. Kwiatkowski, J. Nelson, H. Li, J. L. Bredas, W. Wenzel, C. Lennartz, *Phys. Chem. Chem. Phys.* **2008**, *10*, 1852.

[15] M. Matsumura, Y. Jinde, T. Akai, T. Kimura, *Jpn. J. Appl. Phys.* **1996**, *35*, 5735.

[16] M. Matsumura, K. Furukawa, Y. Jinde, *Thin Solid Films* **1998**, *331*, 96.

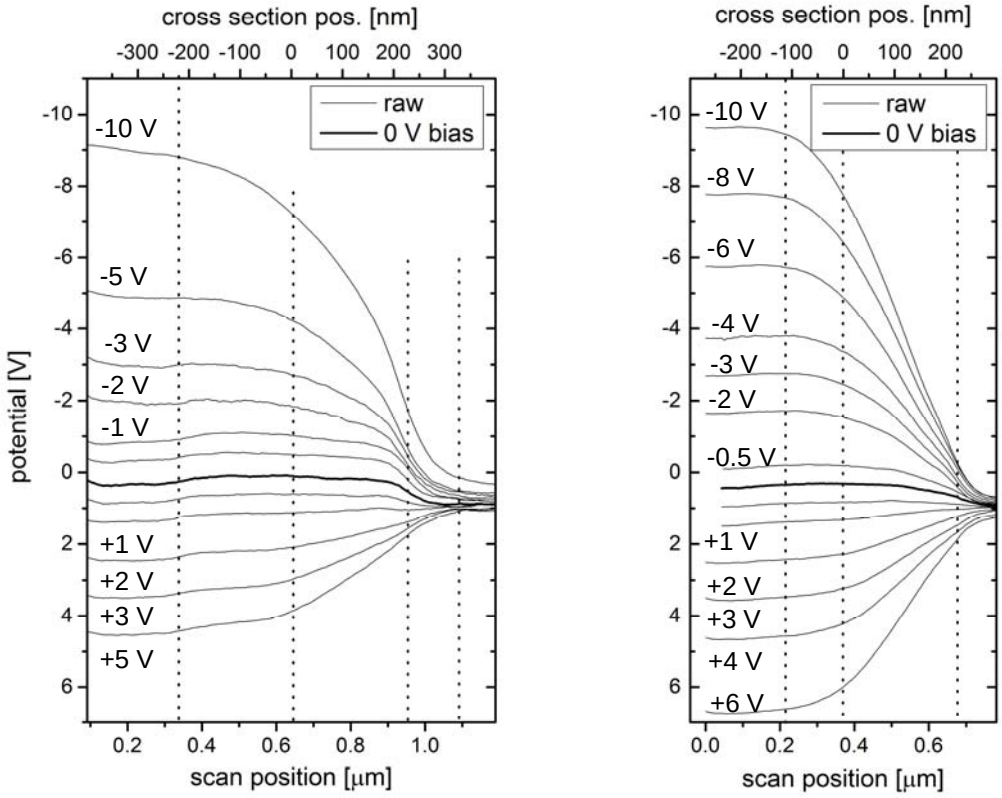

Figure S1 Raw SKPM data within an OLED with an active layer of 224 nm NPB (left), 112 nm NPB (right) and 224 nm Alq_3 at external bias voltage between a) -10 V and 5 V, b) -10 V and +6V. The bold 0 V profiles correspond to the work function difference between the cantilever tip and the sample. Note that final correction for sample drift has not been applied to these curves. The dotted lines represent the approximate location of the interfaces between anode, hole conducting layer, electron conducting layer, cathode (and cathode top - left).

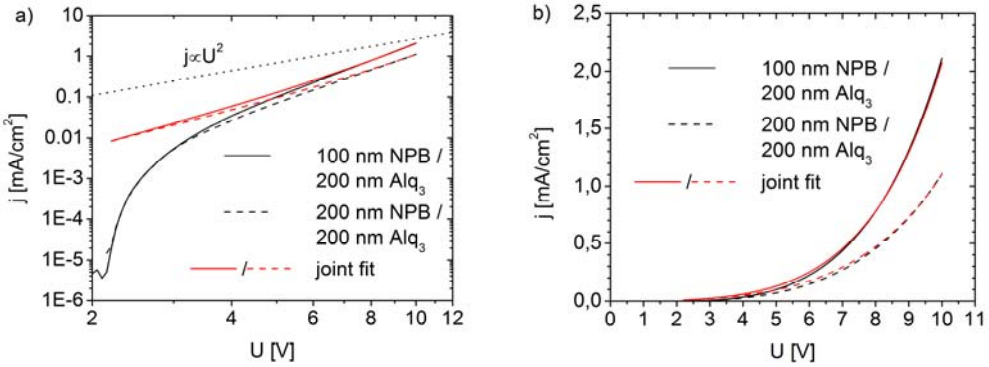

Figure S2 Comparison of experimental I-V curves and the fit of the model proposed by Matsumura et al. in a) logarithmic-logarithmic and b) linear scale. Two free fit parameters (one for the ITO/MoO_3 / NPB interface, one for the built-in voltage between ITO/MoO_3 and LiF/Al) were used. The curves for 100 nm and 200 nm NPB were fitted simultaneously. Deviation at low voltages is expected as the model of Matsumura et al. uses non-zero currents (J0,n) even at zero bias.